

## Optical and dielectric properties of nano BaNbO<sub>3</sub> prepared by a combustion technique

S Vidya<sup>1</sup>, K C Mathai<sup>1</sup>, Annamma John<sup>1</sup>, Sam Solomon<sup>2</sup>, K Joy<sup>1</sup> and J K Thomas<sup>\*1</sup>

<sup>1</sup>Electronic Materials Research Laboratory, Department of Physics, Mar Ivanios College, Thiruvananthapuram 695015, Kerala, India

<sup>2</sup>Dielectric Materials Research Laboratory, Department of Physics, St. John's College, Kollam District, Anchal 691306, Kerala, India

(Received June 29, 2013, Revised February 22, 2013, Accepted March 19, 2013)

**Abstract.** Nanocrystalline Barium niobate (BaNbO<sub>3</sub>) has been synthesized by a novel auto-igniting combustion technique. The X-Ray diffraction studies reveals that BaNbO<sub>3</sub> posses a cubic structure with lattice constant  $a = 4.071 \text{ \AA}$ . Phase purity and structure of the nano powder are further examined using Fourier-Transform Infrared and Raman spectroscopy. The average particle size of the as prepared nano particles from the Transmission Electron Microscopy is 20 nm. The UV-Vis absorption spectra of the samples are recorded and the calculated average optical band gap is 3.74eV. The sample is sintered at an optimized temperature of 1425°C for 2h and attained nearly 98% of the theoretical density. The morphology of the sintered pellet is studied with Scanning Electron Microscopy. The dielectric constant and loss factor of a well-sintered BaNbO<sub>3</sub> at 5MHz sample is found to be 32.92 and  $8.09 \times 10^{-4}$  respectively, at room temperature. The temperature coefficient of dielectric constant was  $-179 \text{ pp/}^\circ\text{C}$ . The high dielectric constant, low loss and negative temperature coefficient of dielectric constant makes it a potential candidate for temperature sensitive dielectric applications.

**Keywords:** combustion synthesis; raman spectroscopy; band gap; dielectric; BaNbO<sub>3</sub>

### 1. Introduction

Niobium based compounds are widely studied by the research community owing to their exceptional optical, electrical, magnetic, dielectric and catalytic properties (Isabella *et al.* 2009, Molina *et al.* 2009, Ensi *et al.* 2012, Han *et al.* 2012, Koduri *et al.* 2012). The interesting physical properties exhibited by the compounds strongly depend on their simple crystalline structure with a large variety of lower symmetry and non stoichiometric oxygen content. Barium niobate belongs to this family of the perovskite structure. The perovskite BaNbO<sub>3</sub> has a high stability and anticorrosion ability. It has been widely used in multilayer ceramic capacitors, chemical sensors, humidity sensors, non volatile memories (Ghosh *et al.* 2007, Venigalla *et al.* 1999, Zhang *et al.* 2009). There are reports that BaNbO<sub>3-x</sub> system with perovskite cubic structure having large oxygen nonstoichiometry exhibit superconductivity although stoichiometric BaNbO<sub>3</sub> is metallic (Strukova

---

\*Corresponding Author, Ph.D., E-mail: [jkthomasemrl@yahoo.com](mailto:jkthomasemrl@yahoo.com).

*et al.* 1997, Gasparov *et al.* 2001).

In microelectronics, they are used as dielectrics, non-linear optical detection devices, in non-volatile ferroelectrics memory (FERAM), substrates for superconducting materials, as sensors and actuators (Vanderbilt *et al.* 1997, Chen *et al.* 2002, Tinte *et al.* 2003, Iles 2007, Tamiko *et al.* 2012, Xuming *et al.* 2012, Donglin *et al.* 2013).

Various techniques have been reported for the synthesis of niobium based compounds with different stoichiometry such as hydrothermal method for barium niobate ultra-fine powders and nanowires (Wu *et al.* 2008), piezoelectric ceramics of  $\text{NaNbO}_3$  and  $\text{KNbO}_3$  by two-step sintering process (Xuming *et al.* 2012), a molten-salt synthesis route for barium iron niobate (Nattaya *et al.* 2012) and a solid-state route from a core-shell structured precursor for the size controlled synthesis of  $\text{KNbO}_3$  (Tamiko *et al.* 2012). In particular, preparation techniques reported for  $\text{BaNbO}_3$  are quick burning solid-state reaction (Strukova *et al.* 1997), pulsed laser ablation (Gasparov *et al.* 2001), ball milling (Chen *et al.* 2006), calcining at high temperature (Casais *et al.* 1995) and composite hydroxide-mediated method (Zhang *et al.* 2009).

However, most of these methods involve high temperature annealing with intermediate grindings in order to obtain an appreciable phase purity which yields large coarse-grained micron sized powders

Single phase barium niobate is very difficult to obtain. In the present work we had synthesized Barium niobate using a modified combustion technique after much optimization of initial conditions. The advantage of this method is that it gives phase pure nano Barium niobate without prolonged heating at high temperatures. The short component diffusion distance at high degree of mixing resulted in lowering of sintering temperature than the studies reported earlier. Among the various techniques for the preparation of nano materials, modified solution combustion route is regarded as one of effective and economic approaches owing to its convenient processing, simple experimental setup, time saving and homogeneity of products (Wariar *et al.* 2012, Vidya *et al.* 2012, Nair *et al.* 2013, Mathai *et al.* 2013).

## 2. Experimental

In a typical modified combustion synthesis, aqueous solution containing ions of Ba and Nb are prepared by dissolving stoichiometric amount of high purity  $\text{Ba}(\text{NO}_3)_2$  (99%, CDH, India) in double distilled water and  $\text{NbCl}_5$  (99%, Alfa Aesar) in hot oxalic acid. Citric acid was added as a complexing agent maintaining the citric acid to the cation ratio at unity. Amount of citric acid was calculated based on total valence of the oxidizing and the reducing agents for maximum release of energy during combustion (Patil *et al.* 2001). Appropriate amount of Urea which acts as fuel was added to the precursor solution. Oxidant/fuel ratio of the system was adjusted by adding conc. nitric acid. The precursor solution is acidic in nature. The solution containing the precursor mixture was heated using a hot plate at  $\sim 250^\circ\text{C}$  in a ventilated fume hood. The solution boils on heating and undergoes dehydration accompanied by foam. The foam gets ignited by itself on persistent heating giving voluminous and fluffy product of combustion. The obtained powder is annealed at oxygen atmosphere at  $600^\circ\text{C}$  in order to eliminate trace amount of organic impurity that may remain in sample and the obtained pure white powder which is characterized as single phase nanocrystals of Barium niobate ceramic.

In the preparation of samples by combustion process, the earlier workers have used poly vinyl

alcohol and urea as the complexing agent and fuel respectively. In such case high temperature annealing of the as-prepared powder was required to get a phase pure powder (Patil *et al.* 2001, Saha and Pramanik 1997). But in the present modified combustion method, citric acid was used as the complexing agent instead of poly vinyl alcohol. By this change of complexing agent it is possible to obtain single phase nanoparticles in a single step combustion process without the usual calcinations for prolonged duration at high temperature. The main advantage of this method is that the as prepared powder itself shows phase formation and the particle size is as low as 20 nm.

Structure of the as-prepared powder was examined by powder X-ray diffraction (XRD) technique using a Bruker D-8 X-ray Diffractometer with Nickel filtered Cu K<sub>α</sub> radiation. The Infrared (IR) spectra of the samples were recorded in the range 400–4000 cm<sup>-1</sup> on a Thermo-Nicolet Avatar 370 Fourier Transform Infrared (FTIR) Spectrometer using KBr pellet method. The Fourier transform–Raman spectrum of the nanocrystalline BaNbO<sub>3</sub> was carried out at room temperature in the wave number range 50–1200 cm<sup>-1</sup> using Bruker RFS/100S Spectrometer at a power level of 150mW and at a resolution of 4 cm<sup>-1</sup>. The samples were excited with an Nd:YAG laser lasing at 1064 nm and the scattered radiations were detected using Ge detector. Particulate properties of the combustion product were examined using transmission electron microscopy (TEM, Model-Hitachi H-600 Japan) operating at 200 kV. The samples for Transmission Electron Microscope (TEM) were prepared by ultrasonically dispersing the powder in methanol and allowing a drop of this to dry on a carbon-coated copper grid. The photoluminescence spectra of the samples were measured using Flurolog<sup>®</sup>-3 Spectrofluorometer. The photons from the source were filtered by an excitation spectrometer. The monochromatic radiation was then allowed to fall on the disc samples and the resulting radiation was filtered by an emission spectrometer and then fed to a photomultiplier detector. The variation of intensity was recorded as a function of wavelength. The absorption spectra were also measured using a Jasco U.V-Visible spectrophotometer.

To study the sinterability of the nanoparticles obtained by the present combustion method, the BaNbO<sub>3</sub> nano particles were mixed with 5% polyvinyl alcohol and pressed in the form of cylindrical pellet of 12 mm diameter and ~ 1.75 mm thickness at a pressure of about 350 MPa using a hydraulic press. The pellet was then sintered at 1425°C for 2h. The sintered density was determined using Archimedes method. The surface morphology of the sintered sample was examined using scanning electron microscopy (SEM) (Model—Hitachi S 2400 Japan). For low frequency dielectric studies the pellets were made in the form of a disc capacitor with the specimen as the dielectric medium. Both flat surfaces of the sintered pellet were polished and then electroded by applying silver paste. The capacitance of the sample was measured using an LCR meter (Hioki-3532-50) for the frequency range 100 Hz - 1MHz.

### 3. Results and discussion

Fig. 1(a) shows the XRD patterns of as prepared Barium niobate nanopowder. The obtained pattern is found to be matching with BaNbO<sub>3</sub> composition reported in the JCPDS file No. 87-0248. All the peaks are indexed for cubic structure having the calculated lattice constant as 4.071Å, which indicate that the formation of BaNbO<sub>3</sub> phase was complete during the combustion process itself without the need for a calcinations step. The crystalline size calculated from full width half maximum (FWHM) using the Scherer formula for the major (011) reflection is found to be ~25 nm.

In the XRD pattern of as prepared sample very small intense peaks can also be seen. These

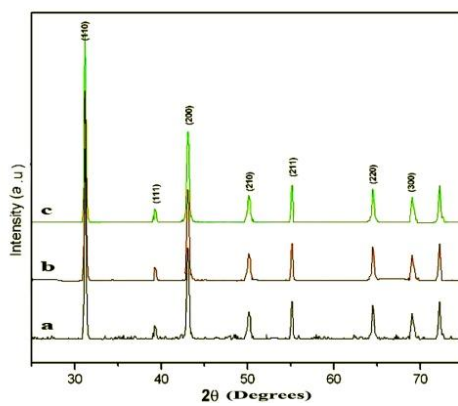


Fig. 1 XRD patterns of (a) as-prepared  $\text{BaNbO}_3$  (b)  $\text{BaNbO}_3$  annealed at  $600^\circ\text{C}$  and (c)  $\text{BaNbO}_3$  heated at  $1200^\circ\text{C}$

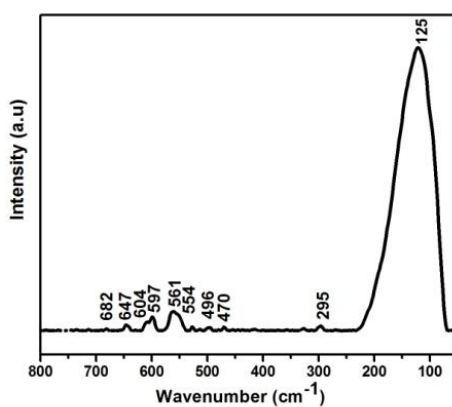


Fig. 2 Raman spectrum of the  $\text{BaNbO}_3$  nano powder annealed at  $600^\circ\text{C}$

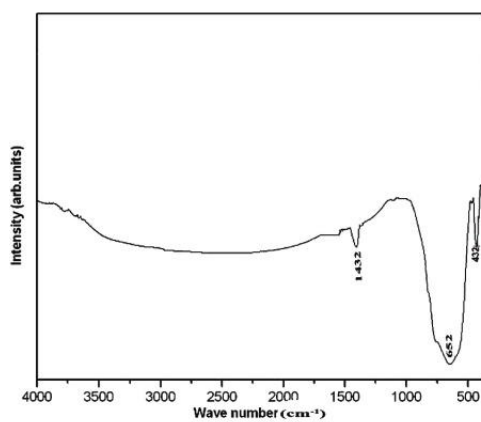


Fig. 3 FT-IR spectrum of the  $\text{BaNbO}_3$  samples annealed at  $600^\circ\text{C}$

reflections are likely due to traces of organic impurities present in the sample as the combustion process takes place in very short duration of time these impurities may remain in the as-prepared sample. To expel this trace amount of impurity the sample was annealed in the range 600°C for 30min. The XRD patterns of a sample heated at 600°C are shown in Fig. 1(b). It is clear from these XRD no peaks other than cubic BaNbO<sub>3</sub> are present. The single phase Barium niobate ceramic is obtained after annealing the as prepared powder at a temperature of 600°C for 30 minutes even though the phase formation was complete during the combustion process itself. The particle size of the sample was increased to 38 nm on annealing at 600°C.

With the intention of finding out any chances of phase transition, the sample was heated at 1200°C for 1hour and XRD of the annealed sample is given as Fig. 1(c). There was no phase transition on heat treatment as there are no appearances or vanishing of peaks. To investigate more on the structural details FT-IR and Raman spectra of the samples were also recorded.

The Raman and FT-IR spectra of the sample annealed at 600°C are given in Figs. 2 and 3 respectively. The observed Raman and IR bands, their relative intensities and the band assignments are shown in Table 1. The nanocrystalline BaNbO<sub>3</sub> has cubic structure with space group Pm3m (*O<sub>h</sub>*), with one molecule in the unit cell. The theoretically predicted vibrational modes of BaNbO<sub>3</sub> at k=0 are given by gives the irreducible representation (Ross 1972, Fateley *et al.* 1972)

$$\Gamma = 3F_{1u} (\text{IR}) + F_{2u} (\text{silent})$$

The compound has no Raman active modes and hence does not give a first order Raman spectrum. However, the recorded Raman spectrum shows certain well defined bands. The observed Raman bands can be assigned on the basis of the vibrations of NbO<sub>6</sub> octahedron, in the distorted perovskite structure. The six fundamental vibrations of the NbO<sub>6</sub> octahedron with *O<sub>h</sub>* symmetry are the symmetrical stretching mode  $\nu_1A_{1g}$ , asymmetric stretching modes  $\nu_2E_g$  and  $\nu_3F_{1u}$ , asymmetric bending mode  $\nu_4F_{1u}$ , symmetric bending mode  $\nu_5F_{2g}$  and the inactive mode  $\nu_6F_{2u}$ .

The three Raman active modes  $\nu_1A_{1g}$ ,  $\nu_2E_g$  and  $\nu_5F_{2g}$  are observed at 682, 561 and 125 cm<sup>-1</sup>, respectively. The  $\nu_1A_{1g}$  mode is observed as a weak band. The  $E_g$  mode is broadened and shows a doublet structure with the other component at 554 cm<sup>-1</sup>. The interference of lattice modes along with  $\nu_5F_{2g}$  mode makes the band at 125 cm<sup>-1</sup> is very strong.

The IR active  $\nu_3F_{1u}$  mode appears as a very strong absorption band at 652 cm<sup>-1</sup> in the absorption spectrum. The medium intense band at 432 cm<sup>-1</sup> in the IR spectrum is due to  $\nu_4F_{1u}$  symmetric bending mode of vibration. Both these IR active modes have become active in Raman spectrum and are observed as triplet or doublet bands in the range 647-597 cm<sup>-1</sup> and 496-470 cm<sup>-1</sup>, respectively. The silent  $\nu_6F_{2u}$  mode is also observed in Raman spectrum at 295 cm<sup>-1</sup>.

Table 1 Raman and IR spectral data of BaNbO<sub>3</sub> and their band assignment

Raman (cm <sup>-1</sup> )	IR (cm <sup>-1</sup> )	Band assignments
682 vw		$\nu_1A_{1g}$
647 m, 604 sh, 597 m, 561 s, 554 sh	652 vs, 771 sh	$\nu_3F_{1u}$
496 w, 470 w	432 m	$\nu_4F_{1u}$
295 w		$\nu_6F_{2u}$
125 vs		$\nu_5F_{2g}$ + Lattice mode

Relative intensities: v-very, s-strong, m-medium, w-weak, sh-shoulder

TEM images of the BaNbO<sub>3</sub> samples prepared via solution combustion processes annealed at 600°C are given in Figs. 4 and 5. TEM image of the as prepared sample shows a spherical morphology with a narrow size of nearly 20 nm. As the temperature increased, the morphology of the powders became faceted approximating to a cuboidal structure with an average particle size of 35 nm. Inset of Fig. 4 shows the selected area electron diffraction (SAED) pattern recorded at an accelerating voltage of 200 kV, which corresponds to an electron wavelength of 2.508 pm and at a camera length of 1.23 m. The BaNbO<sub>3</sub> nanocrystals exhibit sparser rings in the electron diffraction pattern. This is indicative of the polycrystalline nature of the crystallites, but the spotty nature of the SAED pattern can be due to the fact that the finer crystallites having related orientations are agglomerated together resulting in a limited set of orientations.

The UV absorption spectra spectrum of the BaNbO<sub>3</sub> nanoparticles were measured in the range 200-800 nm is shown in the Fig. 6. The absorption spectrum of BaNbO<sub>3</sub> exhibits typical optical behavior of a wide-band gap semiconducting oxide. The absorption spectra include one sharp peak

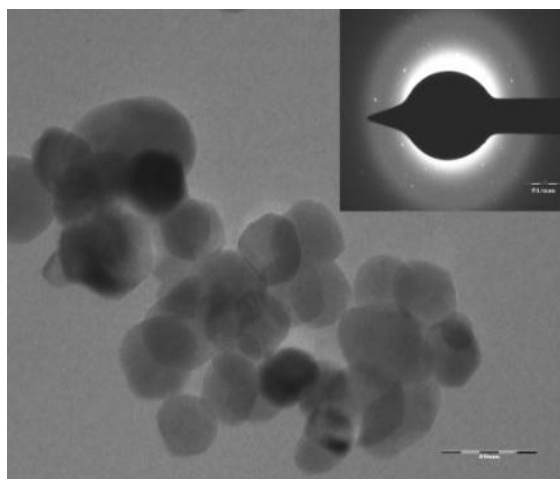


Fig. 4 TEM image of as prepared nano BaNbO<sub>3</sub> samples

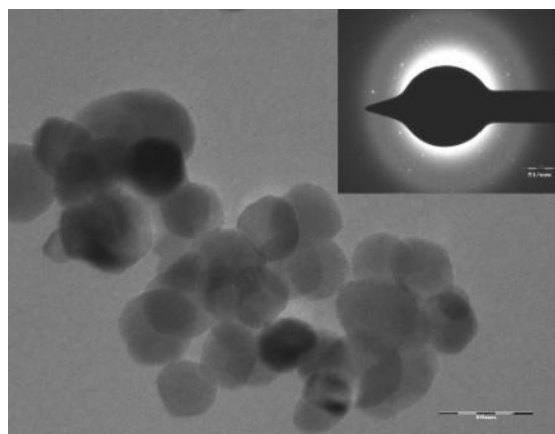
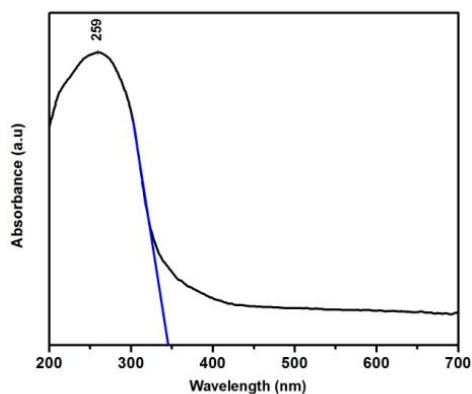
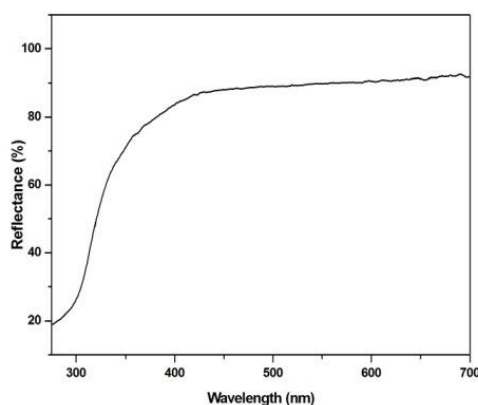


Fig. 5 TEM image of nano BaNbO<sub>3</sub> samples heated at 600°C

Fig. 6 UV-Vis absorption spectra of BaNbO<sub>3</sub> nano particlesFig. 7. Reflectance spectra of BaNbO<sub>3</sub> nano particles

at 259 nm. This indicates that samples absorbs heavily in UV region and moderately in the visible region. The optical absorption in the shorter wavelength region is mainly attributed to the electron transition from the top of the valence band to the bottom of the conduction band (Cahen *et al.* 2000). There is a blue shift in wave length with respect to the early reported value (Zhang 2009) which can be attributed to particle size effect. Usually a blue shift in band gap is expected as particle size reduces because of broadening of the energy levels (Yu *et al.* 2002, Gudiksen *et al.* 2002). This shows that the nano nature of the sample persist even though it was annealed at 600°C for 30minutes. The band gap energy could be determined by extrapolating the wavelength of the onset absorption in UV region as illustrated in the Fig. 6 and solving the relation  $E = hc/\lambda$ . The corresponding band-gap for the wavelength 340nm is 3.64eV.

The reflectance spectra of nano BaNbO<sub>3</sub> is shown in Fig. 7 which indicate maximum reflection in the visible region which decreases towards the UV region where absorption becomes prominent. Such materials found application as UV filters and sensors.

In semiconductors the absorption coefficient near the fundamental edge depends on photo energy. This absorption dependence on photon energy is expressed by the Tauc's equation (Tauc 1974). According to this equation, the optical band gap energy is related with absorbance and photon energy by the following equation:

$$(\alpha h\nu) = \beta(h\nu - E_g)^m$$

where  $\beta$  is an energy independent constant,  $\alpha$  is the optical absorption coefficient,  $h$  is the Planck constant,  $\nu$  is the frequency of incident photon,  $E_g$  is the optical band gap and  $m$  is a constant which characterizes the nature of band transition.  $m=1/2$  and  $3/2$  corresponds to direct allowed and direct forbidden transitions, and  $m=2$  and  $3$  corresponds to indirect allowed and indirect forbidden transitions, respectively. The optical band gap can be obtained from the extrapolation of the straight-line portion of the  $(\alpha h\nu)^{1/m}$  vs  $h\nu$  plot to  $h\nu = 0$ . Fig. 8 shows the Tauc's plot of the BaNbO<sub>3</sub> nanopowder. Thus determined band gap of BaNbO<sub>3</sub> is 3.74eV which is approximately equal to what we got from the absorption spectra itself. This result shows that nano BaNbO<sub>3</sub> is wide band gap semiconductor.

The photo luminescent activity of the sample is investigated by recording the PL emission spectra of sample annealed at 600°C. The photoluminescence spectra obtained at the excitation wavelength 370 nm of the sample is given in Fig. 9. The sample showed good luminescent property in the visible region. It is reported that in the niobium atoms have a d<sup>0</sup> configuration have the d band is empty as all of the d electrons were transferred to the O 2p-band (Kurmaev *et al.* 2002). Thus the emission at 484 nm could be assigned to the recombination of photo excited electrons and holes in the 4d conduction band of Nb and 2p valance band of O. The green emission band at 550 nm is ascribed to structure defects such as distorted NbO<sub>6</sub> octahedral groups (De Araujo *et al.* 1998, Fragoso *et al.* 2005). The degeneracy and splitting of bands in Raman studies also confirms the distortion of NbO<sub>6</sub> octahedron which is also clear from the PL spectral investigations.

The sintering behavior of the nanocrystals of BaNbO<sub>3</sub> powders synthesized through the present combustion route was studied. The BaNbO<sub>3</sub> nanopowder was compressed as cylindrical discs of diameter 12 mm and thickness 5 mm. The relative green density of the specimen used for the sintering study was 55%. The sample was sintered at 1425°C for 2 hours at a rate of 5°C/minute. The density of the sintered sample calculated by Archimedes' method is 98%. The high sintered density for BaNbO<sub>3</sub> pellets derived from nano powder synthesized through the present method may be attributed to enhanced kinetics due to the small degree of agglomeration and ultra fine nature of the powder.

Surface morphology of the sintered sample is analyzed using SEM micrograph shown in Fig. 10. It is evident from the SEM that the sample achieved high densification with little porosity. From the SEM pattern long rectangular sheet like patterns can be seen with their size in the micrometer range. Thus heat treatment resulted in grain growth up to several micrometers. The EDAX pattern of the sintered sample is given in Fig. 11. The EDS analysis shows that all the elements such as barium, niobium and oxygen are present in the sample in the same stoichiometric concentrations and no other impure matter is present.

Dielectric properties such as  $\epsilon_r$  and  $\tan\delta$  of the BaNbO<sub>3</sub> was studied in the frequency range 100 Hz to 5 MHz at room temperature. The dielectric constant  $\epsilon_r$  and loss factor  $\tan\delta$  values of the pellets sintered from the nanopowder, synthesized through the above combustion process were studied in the frequency range 100 Hz to 5 MHz at room temperature with silver electrodes on both sides of the circular disc. Fig. 12 shows variation of  $\epsilon_r$  and  $\tan\delta$  at room temperature with the frequency. The dielectric constant  $\epsilon_r$  and loss factor  $\tan\delta$  values of the BaNbO<sub>3</sub> pellets at 5MHz

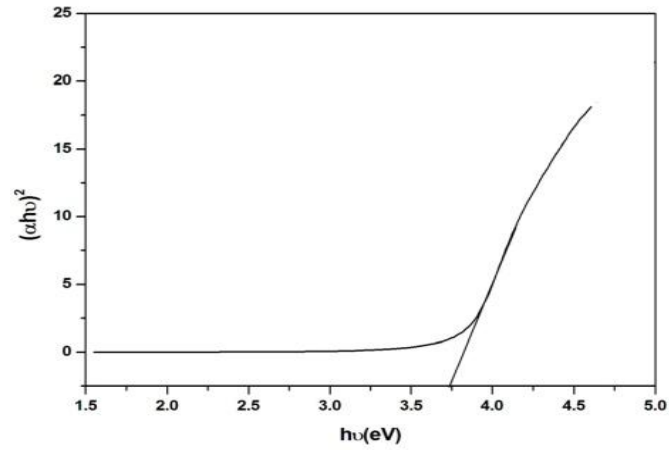


Fig. 8 Tauc's plot of the optical absorption spectrum of BaNbO<sub>3</sub> nanopowder

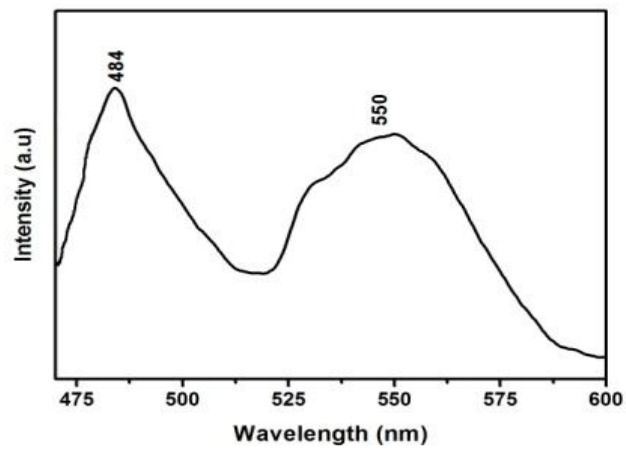


Fig. 9 PL emission spectrum of nano BaNbO<sub>3</sub> annealed at 600°C

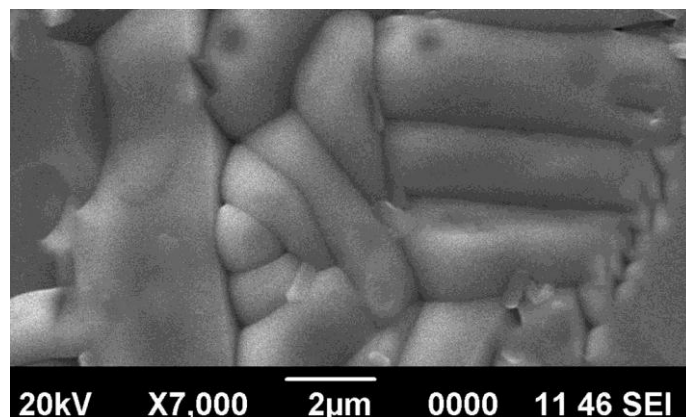


Fig. 10 SEM micrograph of BaNbO<sub>3</sub>

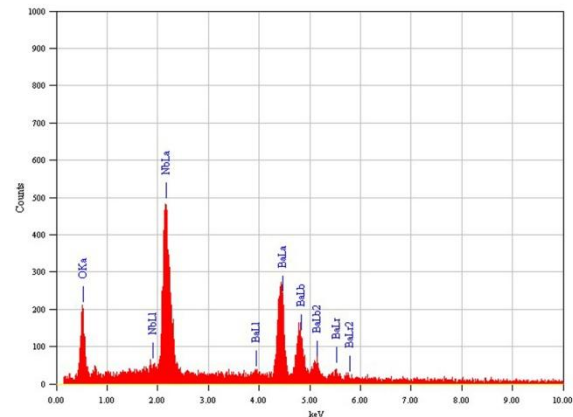


Fig. 11 EDAX pattern of BaNbO<sub>3</sub>

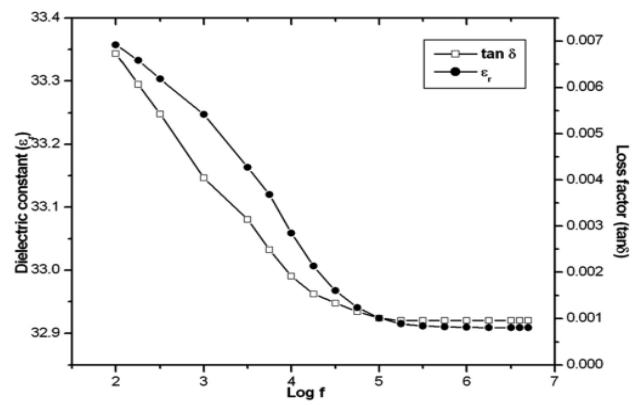


Fig. 12 Variation of  $\epsilon_r$  and  $\tan\delta$  with the frequency

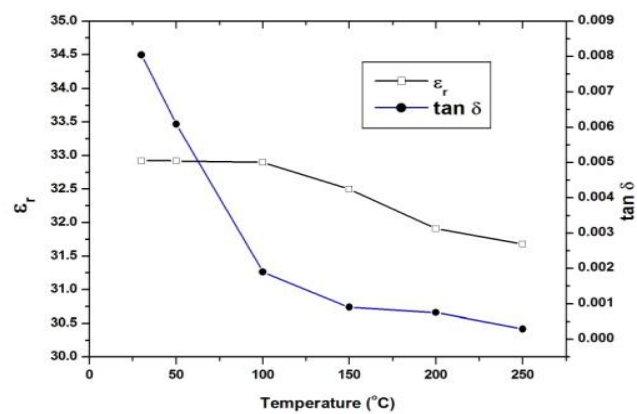


Fig. 13 Variation of  $\epsilon_r$  and  $\tan\delta$  with temperature

were 32.92 and  $8.0905 \times 10^{-4}$  respectively. The values of dielectric constant and very low loss factor indicate the suitability of the sample as a candidate for electronic and dielectric applications.

The variation of  $\epsilon_r$  and  $\tan\delta$  with temperature ranging from 30-250°C is shown in the Fig. 13. It is clear from the graph that the temperature dependence of dielectric constant is very minimal in the measured range. The loss factor decreases with increase of temperature and is of order  $10^{-4}$  at temperature above 100°C. The dielectric constant  $\epsilon_r$  loss factor  $\tan\delta$  of the BaNbO<sub>3</sub> pellets at 5MHz at 250°C are 31.68 and  $2.90 \times 10^{-4}$  respectively.

The temperature coefficient of dielectric constant ( $T_{CK}$ ) is determined using the equation given below between temperature 250°C and 30°C at 5MHz

$$T_{CK} = \left[ \frac{K_{250} - K_{30}}{220 / K_{30}} \right] \times 10^6 \text{ ppm}^\circ\text{C}$$

where  $K_{30}$  and  $K_{250}$  are dielectric constants at 30°C and 250°C respectively, and 220 is the temperature difference. The obtained  $T_{CK}$  is -179 ppm/°C which are negative. Thus nano BaNbO<sub>3</sub> possesses relatively low temperature coefficient of dielectric constant which makes it suitable for temperature dependent dielectric applications.

#### 4. Conclusions

Nanocrystalline semiconducting BaNbO<sub>3</sub> was synthesized through a modified combustion process. The X-ray diffraction studies show that the nanopowder was single phase, crystalline, has BaNbO<sub>3.06</sub> composition with cubic structure having a lattice constant  $a = 4.071 \text{ \AA}$ . TEM and SAED pattern confirms the nanocrystalline nature of the sample. The average particle size of as prepared powder calculated from TEM is 20 nm. FTIR and FT-Raman studies showed that samples possess a distorted cubic perovskite structure. The average of optical band gap determined from the UV-Vis spectrum is 3.74eV. These nanocrystals could be sintered at a relatively low temperature of 1425°C to a high density. The SEM image of the sintered material indicates high densification of the material. The room temperature dielectric constant ( $\epsilon_r$ ) and loss factor ( $\tan\delta$ ) of the sintered pellet at 5 MHz was  $\sim 32.92$  and  $8.0905 \times 10^{-4}$ , respectively indicates the material is suitable for electronic applications. The temperature coefficient of dielectric constant is -179ppm/°C.

#### Acknowledgments

The authors acknowledge University Grants Commission, Council of Scientific and Industrial Research (CSIR), New Delhi for financial supports and Sophisticated Test and Instrumentation Centre (STIC), Cochin University of Science and Technology, Cochin for experimental analysis.

#### References

- Cahan, D., Hodes, G., Grätzel, M., Guillemoles, J.F. and Riess, I. (2000), "Nature of photovoltaic action in dye-sensitized solar cells", *J. Phy. Chem. B.*, **104**(9), 2053-2059.
- Casais, M.T., Alonso, J.A., Rasines, I. and Hidalgo, M.A. (1995), "Preparation, neutron structural study and characterization of BaNbO<sub>3</sub>: A Pauli-like metallic perovskite", *Mater.Res. Bull.*, **30**(2), 201-208.
- Chen, G.H. and Qi, B. (2006), "Barium niobate formation from mechanically activated BaCO<sub>3</sub>-Nb<sub>2</sub>O<sub>5</sub> mixtures", *J. Alloys Compd.*, **425**(1-2), 395-398.

- Chen, Z.X., Chen, Y. and Jiang, Y.S. (2002), "Comparative Study of ABO<sub>3</sub> Perovskite Compounds. 1. ATiO<sub>3</sub> (A = Ca, Sr, Ba, and Pb) Perovskites", *J. Phys. Chem. B.*, **106**(39), 9986-9992.
- De Araujo, A.C.V., Weber, I.T., Fragoso, W.D. and De Mello Donega, C. (1998), "Luminescence and properties of La<sub>2</sub>O<sub>3</sub>-B<sub>2</sub>O<sub>3</sub>-M<sub>2</sub>O<sub>5</sub>:Ln (M=Nb(V) or Ta(V)) and La<sub>2</sub>O<sub>3</sub>-B<sub>2</sub>O<sub>3</sub>-M<sub>2</sub>O<sub>5</sub>-PbO/Bi<sub>2</sub>O<sub>3</sub> glasses", *J. Alloy Compd.*, **275**, 738-741.
- Donglin, G., Hao Hua, C.H. and Yi, X. (2013), "Defect-Induced and UV-Irradiation-Enhanced Ferromagnetism in Cubic Barium Niobate", *J. Phys. Chem. C*, **117** (27), 14281-14288.
- Ensi Cao, Yongjia Zhang, Lin Ju, Lihui Sun and Hongwei Qin, Jifan Hu. (2012), "The investigation of room temperature ferromagnetism in (1 0 0) oriented BaNb<sub>2</sub>O<sub>6</sub> PLD films on LaAlO<sub>3</sub> (1 0 0) substrate", *Appl. Surf. Sci.*, **258**(8), 3795-3799.
- Fateley, W.G., Dollish, F.R., Mc Devitt, N.T. and Benthly, F.F. (1972), *Infrared & Raman selection Rules for molecules & Lattice vibrations: The Correlation Method*, Wiley Interscience, New York.
- Fragoso, W.D., De Mello Donega, C., Longo, R.L., (2005) "A structural model of La<sub>2</sub>O<sub>3</sub>-Nb<sub>2</sub>O<sub>5</sub>-B<sub>2</sub>O<sub>3</sub> glasses based upon infrared and luminescence spectroscopy and quantum chemical calculations", *J Non-Cryst Solids*, **351**, 3121-3126.
- Gasparov, V.A., Ermolov, S.N., Strukova, G.K., Sidorov, N.S., Khassanov, S.S., (2001), "Superconducting and anomalous electron transport properties and electronic structure of BaNbO<sub>3-x</sub> and Ba<sub>2</sub>Nb<sub>5</sub>O<sub>x</sub> films", *Phys. Rev. B.*, **63**(17), 174512-174521.
- Gudiksen, M.S., Wang, J.F., Liebe, C.M. (2002), "Size-Dependent Photoluminescence from Single Indium Phosphide Nanowires", *J. Phys. Chem. B.*, **106**(16), 4036-4039.
- Han, D.F., Zhang, Q.M., Luo, J., Tang, Q., Dun, J. (2012), "Optimization of energy storage density in ANb<sub>2</sub>O<sub>6</sub>-NaNbO<sub>3</sub>-SiO<sub>2</sub> (A=(1-x)Pb, xSr) nanostructured glass-ceramic dielectrics", *Ceram. Int.*, doi.org/10.1016/j.ceramint.2012.04.087.
- Iles, N., Kellou, A., Khodja, K.D., Amrani, B., Lemoigno, F., Bourbie, D. and Aourag, H. (2007), "Atomistic study of structural, elastic, electronic and thermal properties of perovskites Ba(Ti,Zr,Nb)O<sub>3</sub>", *Comp. Mater. Sci.*, **39**(4), 896-902.
- Kinoshita, T., Senna, M., Doshida, Y. and Kishi, H. (2012), "Synthesis of size controlled phase pure KNbO<sub>3</sub> fine particles via a solid-state route from a core-shell structured precursor", *Ceram. Int.*, **38**(3), 1897-1904.
- Kurmaev, E.Z., Moewes, A., Bureev, O.G., Nekrasov, I.A., Cherkashenko, V.M., Korotin, M.A., Ederer, D. L., (2002) "Electronic structure of niobium oxides" *J Alloy Compd*, **347** 213-218
- Koduri, R. and Chandramouli, K. (2012), "Ferroelectric and pyroelectric properties of Ce<sup>3+</sup> modified tetragonal tungsten bronze structured lead barium niobate-55 ceramics", *J. Phys. Chem. Solid.*, **73**(9), 1061-1065.
- Mathai, K.C. Vidya, S. Solomon, S. and Thomas, J.K. (2013), "Variation in Optical, dielectric and sintering behavior of nanocrystalline NdBa<sub>2</sub>NbO<sub>6</sub>", *Adv. Mater. Res., An Intl Journal*, **2** No. 2.
- Molina, P., Martin Rodriguez, E., Jaque, D., Bausa, L.E., Garcia Sole, J., Huaijin Zhang , Wenlan Gao , Jiyang Wang, Minhua Jiang. (2009), "Optical spectroscopy of neodymium-doped calcium barium niobate ferroelectric crystals", *J. Lumin.*, **129**(12), 1658-1660.
- Nair, V.M., Jose, R., Raju, K., Wariar and P.R.S., (2013), "Optimization of citrate complex combustion for synthesis of transition metal oxide nanostructures" *J Alloy. Compds.*, **552**, 180-185.
- Nattaya Tawichai, Waraporn Sittiyot, Sukum Eitssayeam, Kamonpan Pengpat, Tawee Tunkasiri, Gobwute Rujijanagul. (2012), "Preparation and dielectric properties of barium iron niobate by molten-salt synthesis" *Ceram. Int.*, **38S**(1), S121-S124.
- Oprea, I.I., Voelker, U., Niemer, A., Pankrath, R., Podlozhenov, S. and Betzler, K. (2009), "Influence of erbium doping on phase transition and optical properties of strontium barium niobate" *Optl. Mater.*, **32**(1), 30-34.
- Patil, R.C., Radhakrishnan, S., Sushama, P. and Vijaymohanan, K. (2001), "Piezoresistivity of conducting polyaniline/BaTiO<sub>3</sub> composites", *J. Mater. Res.*, **16**(07), 1982-1988.
- Ross, S.D. (1972), *Inorganic Infrared and Raman Spectra*, Mc Graw Hill Book Company, London.,
- Saha, S.K. and Pramanik (1997), "Synthesis of nanophase PLZT (12/40/60) powder by PVA-solution

- technique”, *Nanostruct. Mater.*, **8**(1), 29-36.
- Strukova, G.K., Kedrov, V.V., Zverev, V.N., Khasanov, S.S., Ovchinnikov, I.M., Batov, I.E. and Gasparov, V.A. (1997), “On the synthesis and the electric and magnetic properties of superconducting barium–niobium–oxide compounds”, *Physica C.*, **291** (3-4), 207-212.
- Ghosh, S., Dasgupta, S., Sen, A. and Maiti, H.S. (2007), “Synthesis of barium titanate nanopowder by a soft chemical process”, *Mater. Lett.*, **61**(2), 538-541.
- Tauc, J. (1974), *Amorphous and liquid semiconductors*, Plenum, New York.
- Tinte, S., Iniguez, J., Rabe, K.M. and Vanderbilt, D. (2003), “Quantitative analysis of the first-principles effective Hamiltonian approach to ferroelectric perovskites”, *Phys. Rev. B.*, **67**(6), 64106-64114.
- Vanderbilt, D. (1997), “First-principles based modelling of ferroelectrics”, *Curr. Opin. Solid St. M.*, **2**(6), 701-705.
- Venigalla, S. (2001), “Barium titanate advanced materials and powders”, *Am. Ceram. Soc. Bull.*, **6**, 63-64.
- Vidya, S., John, A., Solomon, S. and Thomas, J.K. (2012), “Optical and dielectric properties of SrMoO<sub>4</sub> powders prepared by the combustion synthesis method”, *Adv. Mater. Res. An Intl. Journal*, **1**, 3
- Wariar, P.R.S., Kumar, V.R., Nair, V.M., Yusoff, M.M., Jose R. and Koshy J. (2012), “Nanostructured A<sub>2</sub>(RE,B)O<sub>6</sub> (A = Ba, Sr; RE = Rare-Earth; B = Sb, Zr) Perovskite Ceramics and their Potential Applications in Microwave and Superconducting Electronics”, *Adv.Mater.Res.*, **545**, 27-31.
- Wu, S.Y., Chen, X.M. and Liu, X.Q. (2008), “Hydrothermal derived barium niobate ultra-fine powders and nanowires”, *J. Alloy .Compd.*, **453**(1-2), 463-469.
- Xuming, P., Jinhao, Q., Kongjun, Z. and Jianzhou, D. (2012) “(K, Na)NbO<sub>3</sub>-based lead-free piezoelectric ceramics manufactured by two-step sintering”, *Ceram.Int.*, **38**(3), 2521-2527
- Yu, D.P., Bubendorff, J.L., Zhou, J.F., Wang, Y.L. and Troyon, M. (2002), “Localized cathodoluminescence investigation on single Ga<sub>2</sub>O<sub>3</sub> nanoribbon/nanowire”, *Solid State Commun.*, **124**(10-11), 417-421.
- Zhang, M., Hu, C., Liu, H., Xiong, Y. and Zhang, Z. (2009), “A rapid-response humidity sensor based on BaNbO<sub>3</sub> nanocrystals”, *Sensor. Actuat. B.Chem.*, **136**(1), 128-132.